Nitric Oxide Chemistry

International Edition: DOI: 10.1002/anie.201605705
German Edition: DOI: 10.1002/ange.201605705

Mechanistic Insight into the Nitric Oxide Dioxygenation Reaction of Nonheme Iron(III)–Superoxo and Manganese(IV)–Peroxo Complexes

Seungwoo Hong[+], Pankaj Kumar[+], Kyung-Bin Cho[+], Yong-Min Lee, Kenneth D. Karlin, and Wonwoo Nam**

Abstract: *Reactions of nonheme Fe^{III}–superoxo and Mn^{IV}–peroxo complexes bearing a common tetraamido macrocyclic ligand (TAML), namely $[(TAML)Fe^{III}(O_2)]^{2-}$ and $[(TAML)Mn^{IV}(O_2)]^{2-}$, with nitric oxide (NO) afford the Fe^{III}–NO_3 complex $[(TAML)Fe^{III}(NO_3)]^{2-}$ and the Mn^{V}–oxo complex $[(TAML)Mn^{V}(O)]^{-}$ plus NO_2^-, respectively. Mechanistic studies, including density functional theory (DFT) calculations, reveal that M^{III}–peroxynitrite (M = Fe and Mn) species, generated in the reactions of $[(TAML)Fe^{III}(O_2)]^{2-}$ and $[(TAML)Mn^{IV}(O_2)]^{2-}$ with NO, are converted into $M^{IV}(O)$ and $^{\bullet}NO_2$ species through O–O bond homolysis of the peroxynitrite ligand. Then, a rebound of $Fe^{IV}(O)$ with $^{\bullet}NO_2$ affords $[(TAML)Fe^{III}(NO_3)]^{2-}$, whereas electron transfer from $Mn^{IV}(O)$ to $^{\bullet}NO_2$ yields $[(TAML)Mn^{V}(O)]^{-}$ plus NO_2^-.*

Mononuclear metal complex/nitric oxide (NO) interactions are of great interest, since NO has been discovered to play major roles in many biophysiological processes, including vascular regulation, neurotransmission, and the immune response.[1] In this context, the biosynthesis of NO and its various biological and physiological reactivities come about through interaction with metalloproteins containing iron and/or copper.[2] However, NO itself is highly toxic because of its radical character and ability to form reactive nitrogen species (RNS) such as $^{\bullet}NO_2$ and peroxynitrite (PN, $O{=}NOO^-$). These RNS may result from NO oxidation in the presence of O_2, H_2O_2, or superoxide radicals, and/or through transition-metal-mediated oxidation.[3–6] RNS have attracted great interest since they play important roles in many biological reactions associated with aging or disease development.[3] RNS, like PN and/or $^{\bullet}NO_2$, can effect tyrosine nitration in proteins,[3,6] and therefore can be responsible for enzyme damage and inactivation;[7] tyrosine or fatty acid nitration reactions may also function in cell signaling.[3f,g,8]

Since the presence of RNS can lead to harmful consequences, aerobic and anaerobic organisms have developed mechanisms to scavenge nitric oxide. Anaerobic bacterial heme-containing NO reductases (NORs)[2d,9] effect NO detoxification by carrying out reductive coupling to N_2O, whereas nonheme diiron proteins are known to catalyze the NOR reaction in many different bacteria and archaea.[10] Under aerobic conditions, the appropriate NO level (in vivo) is maintained by nitric oxide dioxygenases (NODs); widely occurring NODs are microbial or mammalian heme proteins [e.g., hemoglobin (Hb) or myoglobin (Mb)] that catalyze the conversion of toxic NO into biologically benign nitrate ions (NO_3^-).[2a,11] Herein, it is proposed that oxyhemes (e.g., iron(III)–superoxo species) react with NO to form iron–PN intermediates $[Fe^{III}(^{-}OON{=}O)]$.[11] A ferryl species $[Fe^{IV}(O)]$ plus an NO_2 radical then forms through homolytic O–O bond cleavage of the PN fragment, and subsequent formation of a new N–O bond gives the (heme)Fe^{III}–nitrate product.[12] In biomimetic studies, Groves and co-workers reported time-resolved spectrophotometric evidence for the formation of ferryl plus NO_2 in the reaction of met-Mb with PN.[12] On the other hand, Pacheco and co-workers showed that the complementary heme/O_2 + NO reaction may not produce such intermediates.[13] In any case, a heme–PN moiety has not been directly detected; its lifetime is expected to be very short prior to the very rapid rearrangement to produce the NO_3^- product.[14]

To mimic NOD reactivity, we recently reported the reactions of superoxide and peroxide complexes of chromium–TMC (TMC = N-tetramethylated cyclam) with NO; the Cr^{III}–peroxo complex $[(12\text{-TMC})Cr^{IV}(O_2)(Cl)]^+$ reacted with NO to form a Cr^{III}–nitrato complex,[15a] whereas a reaction of the Cr^{III}–superoxo complex $[(14\text{-TMC})Cr^{III}(O_2)(Cl)]^+$ and NO gave the Cr^{IV}–oxo complex ($[(14\text{-TMC})Cr^{IV}(O)(Cl)]^+$) plus $^{\bullet}NO_2$.[15b] We have also reported a NOD reaction using an Fe^{III}–peroxo complex and nitrosonium ion (NO^+), which produced an Fe^{III}–nitrato complex.[15c]

As alluded to above, it has been proposed that iron(III)–superoxo species are key intermediates that react with NO in the reactions of NODs; however, isolated and/or well-characterized iron(III)–superoxo complexes have rarely been used in NO dioxygenation reactions.[14] This is probably due to the high reactivity and thermal instability of synthetic iron(III)–superoxo complexes. Recently, we reported the synthesis, isolation, and structural and spectroscopic characterization of thermally stable mononuclear nonheme iron(III)–superoxo and manganese(IV)–peroxo complexes bearing a common tetraamido macrocyclic ligand (TAML), namely $[(TAML)Fe^{III}(O_2)]^{2-}$ (**1**) and $[(TAML)Mn^{IV}(O_2)]^{2-}$ (**2**; Scheme 1).[16] This provided us with an opportunity to use these isolated metal–oxygen complexes for the study of NO reactions. Herein, we report that reactions of **1** and **2** with

[*] Dr. S. Hong,[+] Dr. P. Kumar,[+] Dr. K.-B. Cho,[+] Dr. Y.-M. Lee, Prof. Dr. W. Nam
Department of Chemistry and Nano Science
Ewha Womans University, Seoul 03760 (Korea)
E-mail: wwnam@ewha.ac.kr
Prof. Dr. K. D. Karlin
The Johns Hopkins University, Baltimore, MD 21218 (USA)
E-mail: karlin@jhu.edu
[+] These authors contributed equally to this work.

Supporting information for this article can be found under: http://dx.doi.org/10.1002/anie.201605707.

 © 2016 Wiley-VCH Verlag GmbH & Co. KGaA, Weinheim

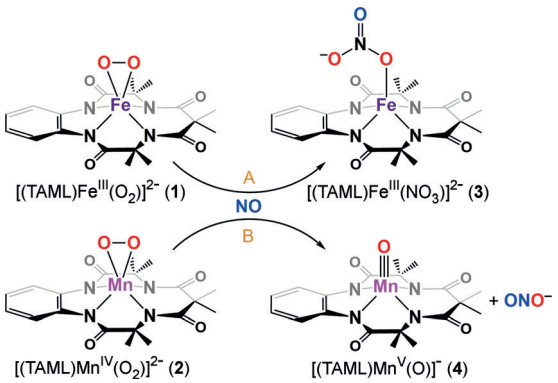

Scheme 1. Reactions of NO with $[(TAML)Fe^{III}(O_2)]^{2-}$ (**1**; reaction A) and $[(TAML)Mn^{IV}(O_2)]^{2-}$ (**2**; reaction B).

NO afford the Fe^{III}–nitrato complex $[(TAML)Fe^{III}(NO_3)]^{2-}$ and the Mn^{V}–oxo complex $[(TAML)Mn^{V}(O)]^{-}$ plus NO_2^-, respectively (Scheme 1). Mechanisms for the formation of the Fe^{III}–nitrato and Mn^{V}–oxo complexes are proposed on the basis of chemical studies accompanied by density functional theory (DFT) calculations, such as O–O bond homolysis of putative M^{III}–peroxynitrite (M = Fe and Mn) intermediates to generate $M^{IV}(O)$ and $^{\bullet}NO_2$ species, and subsequent alternative pathways for the formation of differing final products (i.e., Fe^{III}–nitrato vs. Mn^{V}–oxo species).

For the reaction of $[(TAML)Fe^{III}(O_2)]^{2-}$ with NO, the Fe^{III}–superoxo complex $[(TAML)Fe^{III}(O_2)]^{2-}$ (**1**) was synthesized and isolated according to the reported method.[16] When **1** was reacted with 1.0 equiv of $NO_{(g)}$ under an Ar atmosphere in CH_3CN at −40 °C (see the Experimental Section in the Supporting Information), it was converted into a new species, denoted as **3**, over approximately 5 min. The characteristic absorption bands of **1** at 400 and 490 nm disappeared and a new absorption band at 360 nm appeared with isosbestic points at 330, 388, 430, and 464 nm (Figure 1 a). Then, **3** was analyzed with various spectroscopic methods and X-ray crystallography. The electrospray ionization mass spectrum (ESI-MS) of **3** exhibited a prominent ion peak at *m*/*z* 426.2 (Figure 1 a, inset), the mass and isotope distribution pattern of which correspond to $[Fe^{III}(TAML)]^-$ (calcd *m*/*z* 426.1). An electron paramagnetic resonance (EPR) spectrum of **3** exhibited signals at $g = 3.9$ and 2.02 in CH_3CN at 5 K (Figure S1 in the Supporting Information), which result from an intermediate-spin ($S = 3/2$) d^5 Fe^{III} ion. An infrared (IR) spectrum of **3** showed a strong band at 1385 cm^{-1}, which is assignable to a NO_3^- ion bound to an Fe^{III} center (Figure S2, see below).[17] Finally, the structure of **3** was determined by X-ray crystallography. An authentic compound of **3** was synthesized independently by reacting $[Fe^{III}(TAML)]^-$ with tetrabutylammonium nitrate and comparing the spectroscopic data of **3** with those of the authentic compound (see the Experimental Section in the Supporting Information; also see Tables S1 and S2 and Figures S1, S3, and S4). In addition, a quantitative estimation of NO_3^- ions formed in the reaction of **1** and NO was conducted by using a modified Griess assay by adding VCl_3,[18] and the results indicated that the yield of **3** was 87(5)% based on the amount of NO_3^- ions present in the reaction product solution (Experimental Section in the

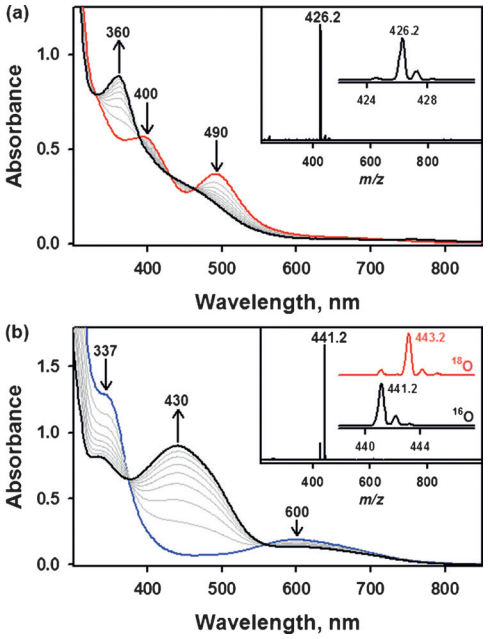

Figure 1. a) UV/Vis spectral changes for **1** (0.15 mM) upon addition of 1.0 equiv of NO in CH_3CN at −40 °C under an Ar atmosphere (**1** red line; **3** black line). Inset: ESI-MS spectrum of **3**. b) UV/Vis spectral changes for **2** (0.25 mM) upon addition of 1.0 equiv of NO in CH_3CN at −40 °C under an Ar atmosphere (**2** blue line; **4** black line). Inset: ESI-MS spectrum of **4**: **4**-^{16}O (black) and **4**-^{18}O (red).

Supporting Information and Figure S5). On the basis of the spectroscopic and structural characterization of **3**, we conclude that the reaction of this Fe^{III}–superoxo complex with NO yielded the Fe^{III}–nitrato complex $[Fe^{III}(TAML)(NO_3)]^{2-}$ as a product (see the proposed mechanism depicted in Scheme 2).

We also investigated the reaction of $NO_{(g)}$ with the Mn^{IV}–peroxo complex $[(TAML)Mn^{IV}(O_2)]^{2-}$ (**2**),[16] which has an isoelectronic structure to the Mn^{III}–superoxo complex $[(TAML)Mn^{III}(O_2)]^{2-}$. The Mn^{IV}–peroxo complex (**2**) was synthesized and isolated according to the reported method,[16] and we used the isolated Mn^{IV}–peroxo complex for the reactions in this study. Upon addition of an equal amount of $NO_{(g)}$ to a solution of **2** under an Ar atmosphere in CH_3CN at −40 °C (see the Experimental Section in the Supporting Information), we observed the formation of a new species, denoted as **4**, within approximately 1 min. An increase of an absorption band at 430 nm was observed along with clean isosbestic points at 366 and 558 nm (Figure 1 b). The reaction rate increased with an increase in the relative concentration of $NO_{(g)}$ (Figure S6a), thus suggesting that the formation of the Mn^{III}–peroxynitrite species in the reaction of **2** and NO is a rate-determining step (rds; Scheme 2, pathway *b*). The reaction rate for **2** and NO was determined to be $1.1 \times 10^3\ M^{-1}s^{-1}$ under second-order reaction conditions (Figure S6b). Based on spectroscopic analysis using ESI-MS, EPR, and IR, and comparing its spectroscopic data with those of an authentic compound prepared independently by reacting $[Mn^{III}(TAML)]^-$ with iodosylbenzene (PhIO), **4** was assigned as the high-valent Mn^{V}–oxo complex $[(TAML)Mn^{V}(O)]^-$.[19] ESI-MS of **4** revealed a prominent ion peak at *m*/*z*

 © 2016 Wiley-VCH Verlag GmbH & Co. KGaA, Weinheim

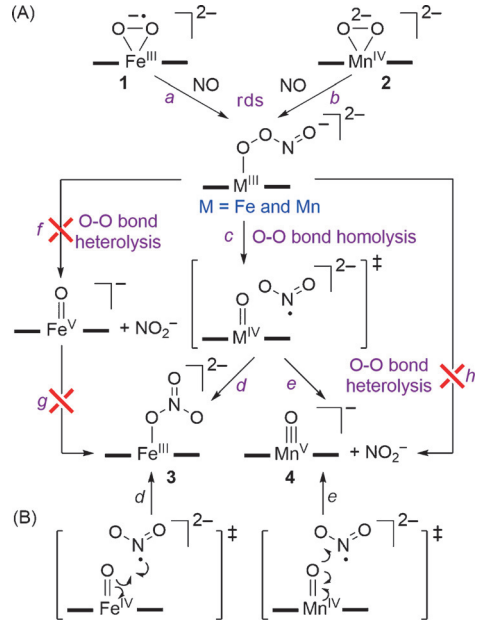

Scheme 2. Proposed mechanisms illustrating the formation of different products in the reactions of $[(TAML)Fe^{III}(O_2)]^{2-}$ (**1**) and $[(TAML)Mn^{IV}(O_2)]^{2-}$ (**2**) with NO.

441.2 (Figure 1 b, inset), the mass and isotope distribution pattern of which correspond to $[(TAML)Mn(O)]^-$ (calcd *m/z* 441.1). When ^{18}O-labeled **2** (i.e., $[(TAML)Mn^{IV}(^{18}O_2)]^{2-}$) was used in the reaction with NO, a prominent ion peak at *m/z* 443.2 was obtained in the ESI-MS of **4** (Figure 1 b, inset), thus demonstrating that the source of the oxygen atom in the manganese–oxo product (**4**) was the ^{18}O-labeled manganese–peroxo complex. Compound **4** was EPR silent, which is consistent with the oxidation state of Mn^V (Figure S7). An IR spectrum of the isolated products obtained from the reaction of **2** and NO showed a strong band at 1277 cm^{-1} resulting from NO_2^- ions (Figure S8; see below). In addition, the yield of NO_2^- ions formed in the reaction of **2** with NO was determined to be 90(4)% by using a Griess assay (see the Experimental Section in the Supporting Information and Figure S9), which is consistent with that determined from the absorbance at 430 nm of the authentic compound **4** in UV/Vis measurements ($\varepsilon = 4000\,M^{-1}cm^{-1}$ of the authentic compound **4**).[19] We therefore conclude that the high-valent Mn^V–oxo species $[(TAML)Mn^V(O)]^-$ (**4**) is formed quantitatively in the reaction of $[(TAML)Mn^{IV}(O_2)]^{2-}$ and NO (see below for a discussion of a proposed mechanism in Scheme 2).

How are the products, such as $[Fe^{III}(TAML)(NO_3)]^{2-}$ without an oxo ligand versus $[Mn^V(TAML)(O)]^-$ with an oxo ligand, formed in the reactions of **1** and **2**, respectively, with $NO_{(g)}$ (Scheme 1)? It is proposed that Fe^{III}–peroxynitrite (Fe^{III}–PN) and Mn^{III}–peroxynitrie (Mn^{III}–PN) are generated in the reactions of both **1** and **2** with NO (Scheme 2 A, reaction pathways *a* and *b*).[20] Since the Fe^{III}–PN and Mn^{III}–PN species are not detected due to their high reactivity and instability, and we do not observe any intermediates after these species are presumed to be formed, we investigated the reaction pathways of the Fe^{III}–PN and Mn^{III}–PN species by carrying out DFT calculations (Tables S3–S20). The result was that the actual formation of the metal–PN species by addition of NO to **1** and **2** was found to be very facile (Tables S4 and S7). In the case of an Fe^{III}–PN species, the ground spin state is calculated to be $S = 3/2$ (Figure 2). The

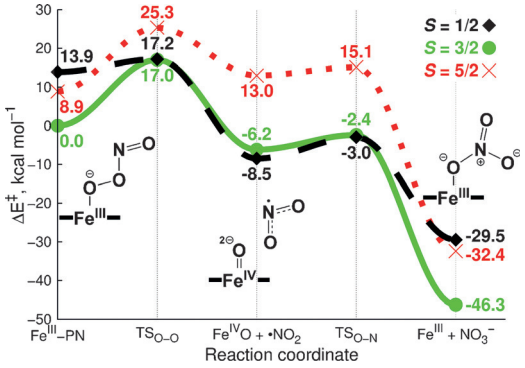

Figure 2. Energy profile of the reaction of **1** and NO, as calculated from DFT. The reaction is proposed to proceed wholly in the $S = 3/2$ state, since there are no particular energetic reasons to perform this reaction in other spin states.

reaction then goes through an O–O bond-breaking step (Scheme 2 A, pathway *c*), with an energy barrier of 17.0 kcal mol^{-1} ($TS_{O\text{-}O}$), that leads to an $Fe^{IV}O$ intermediate and $^{\bullet}NO_2$ formation. The spin-density distribution on Fe and O is 1.5 and 0.5, respectively (Table S11). This is somewhat different from what is usually obtained theoretically in $Fe^{IV}O$ systems with other ligands (1.0 on both Fe and O), but it nevertheless clearly represents an $Fe^{IV}O$ species since the NO_2 formed is a radical species (Table S11). This rules out alternative reaction mechanisms, such as the formation of $[Fe^{III}(TAML)]^-$ and NO_3^- through O–O bond heterolysis (Scheme 2 A, reaction pathways *f* and *g*). This was further verified by experiments, in which no formation of $[(TAML)Fe^V(O)]^-$ was observed in the reaction of **1** and NO (Scheme 2, reaction pathways *a* and *f*). In addition, when $[(TAML)Fe^V(O)]^-$ was synthesized independently and reacted with NO_2^-, no formation of $[Fe^{III}(TAML)]^-$ and NO_3^- was observed (Scheme 2 A, reaction pathway *g*; Figure S10). The theoretical and experimental results thus clearly rule out a heterolytic O–O bond cleavage pathway for the formation of **3** from a presumed Fe^{III}–PN species (Scheme 2 A, reaction pathways *f* and *g*).

Homolytic O–O bond cleavage to form the $^{\bullet}NO_2$ radical ensures a fast rebound FeO–NO_2 bond-formation step over a minor barrier ($TS_{O\text{-}N}$, Figure 2, Scheme 2 B, left panel). Thus, the product formed is $[(TAML)Fe^{III}(NO_3)]^{2-}$ (Scheme 2 A, reaction pathway *d*), as evidenced by the experimental data. From an energetics point of view, the whole reaction can be done on the $S = 3/2$ spin-state pathway. Although the $S = 1/2$ state exhibits a similar energy profile with a slightly more stable $Fe^{IV}O$ intermediate, its higher energies at the beginning and end points of the reaction render it unnecessary for the reaction to switch spin states since there is virtually no energetic advantage in doing this. The $S = 5/2$ state is ruled out due to high energies throughout the course of the reaction (see Figure 2).

 © 2016 Wiley-VCH Verlag GmbH & Co. KGaA, Weinheim

In the case of Mn^{III}–PN species, one can envision a reaction mechanism similar to that for **1** with NO at the initial stage. After a Mn^{III}–PN species is formed through nucleophilic attack of **2** on NO (Scheme 2A, pathway *b*), homolytic O–O bond cleavage of the PN ligand would result in the generation of a thermodynamically unstable $Mn^{IV}O$ complex and $^{\bullet}NO_2$ (Scheme 2A, pathway *c*). However, unlike in the case of **1** with NO, our experimental results indicate that the $Mn^{IV}O$ species does not react further with $^{\bullet}NO_2$ to form Mn^{III} and NO_3^-. Instead, an electron is transferred from $Mn^{IV}O$ to $^{\bullet}NO_2$, to form the thermodynamically more stable $Mn^{V}O$ (**4**) and NO_2^- species (Scheme 2A, reaction pathway *e*; Scheme 2B).

DFT calculations show an energy profile supporting this reaction mechanism. The Mn^{III}–PN species was found to possess an $S=2$ spin state, with an O–O bond-breaking transition state at 14.9 kcal mol^{-1} (Figure 3). This transition

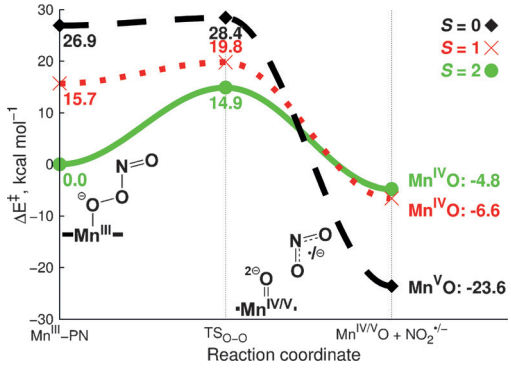

Figure 3. Energy profile of the reaction of **2** and NO, as calculated from DFT. While the reaction starts and is mediated at the $S=2$ state, a switch to the $S=0$ state at the end of the reaction affords the $Mn^{V}O$ and NO_2^- products, which is accompanied by an energy gain of 18.8 kcal mol^{-1}.

state is lowest in energy among all of the spin states; this fact alone thus makes the reaction unlikely to occur in any other spin states. The products, $Mn^{IV}O$ species and $^{\bullet}NO_2$, are now 4.8 kcal mol^{-1} under the starting point. Unlike in the Fe case, however, Mn has an electron configuration that allows a stable $Mn^{V}O$ species to form. While the $S=0$ spin state is unlikely to mediate the heterolytic O–O bond-breaking reaction due to high barriers ($TS_{O\text{-}O}$, Figure 3; Scheme 2A, reaction pathway *h*), the resulting $Mn^{IV}O$ species from the $S=2$ reaction could release an electron to $^{\bullet}NO_2$ with a concomitant spin flip (Scheme 2A, reaction pathway *e*; Scheme 2B). The incentive for the reaction to undergo this electron transfer and spin flip lies in the exogenicity of this reaction, which forms an $S=0$ $Mn^{V}O$ and NO_2^- species while gaining 18.8 kcal mol^{-1} in energy. Simple model calculations would put a similar reaction with $Fe^{IV}O$ turning into $Fe^{V}O$ as endogenic by 2.0 kcal mol^{-1} (data not shown). This reaction would thus not be competitive with forming Fe^{III} and NO_3^- instead, a reaction that is exogenic by 40.1 kcal mol^{-1} (Figure 2).

In summary, we have investigated the NO reactions of metal–O_2 complexes to provide further insight into fundamental aspects of NOD chemistry. Such reactions are important in the biological regulation of nitric oxide and they involve transition-metal complexes and species derived from molecular oxygen and/or nitric oxide. We have shown that the reaction of the iron(III)–superoxo complex $[(TAML)Fe^{III}(O_2)]^{2-}$ with NO yields the Fe^{III}–NO_3 product $[(TAML)Fe^{III}(NO_3)]^{2-}$, which is most likely formed through an Fe^{III}–PN intermediate and homolytic O–O bond cleavage of the Fe^{III}–PN species to form $Fe^{IV}O$ and $^{\bullet}NO_2$ products (Scheme 2). The present result is one of the very few examples of using isolated and well-characterized iron(III)–superoxo complexes in biomimetic studies of NOD enzymes, such as Hb and Mb.[9–12] In contrast, the corresponding manganese complex $[(TAML)Mn^{IV}(O_2)]^{2-}$, which has an isoelectronic structure to the Mn^{III}–superoxo complex $[(TAML)Mn^{III}(O_2)]^{2-}$, shows a different reactivity; the reaction of $[(TAML)Mn^{IV}(O_2)]^{2-}$ with NO produces $[(TAML)Mn^{V}(O)]^-$ and NO_2^-. DFT calculations attribute this different behavior to the electron configuration of the $Mn^{V}O$ species, which is highly stable in its $S=0$ mode; a transient $Mn^{IV}O$ species releases an electron to $^{\bullet}NO_2$ with a concomitant spin flip. The present results describe original findings in that structurally comparable complexes that mediate the formation and subsequent transformation of peroxynitrite can undergo varying reaction mechanisms to give rise to different products, depending on the identity of the metal ion and the electron configuration (and/or spin state).

Acknowledgements

The authors gratefully acknowledge research support of this work by the NRF of Korea through CRI (NRF-2012R1A3A2048842 to W.N.), GRL (NRF-2010-00353 to W.N.), and MSIP of Korea (NRF-2013R1A1A2062737 to K.-B.C.), along with the USA National Institutes of Health (to K.D.K.).

Keywords: biomimetic chemistry · iron · manganese · nonheme metal–oxo complexes · reactive nitrogen species

How to cite: *Angew. Chem. Int. Ed.* **2016**, *55*, 12403–12407
Angew. Chem. **2016**, *128*, 12591–12595

[1] a) J. E. Ignarro, *Nitric Oxide, Biology and Pathobiology*, Academic Press, San Diego, CA, **2000**; b) G. B. Richter-Addo, P. Legzdins, J. Burstyn, *Chem. Rev.* **2002**, *102*, 857; c) I. M. Wasser, S. de Vries, P. Moënne-Loccoz, I. Schröder, K. D. Karlin, *Chem. Rev.* **2002**, *102*, 1201; d) J. K. S. Møller, L. H. Skibsted, *Chem. Rev.* **2002**, *102*, 1167.

[2] a) M. P. Doyle, J. W. Hoekstra, *J. Inorg. Biochem.* **1981**, *14*, 351; b) C. E. Cooper, J. Torres, M. A. Sharpe, M. T. Wilson, *FEBS Lett.* **1997**, *414*, 281; c) E. I. Tocheva, F. I. Rosell, A. G. Mauk, M. E. P. Murphy, *Science* **2004**, *304*, 867; d) N. Lehnert, T. C. Berto, M. G. I. Galinato, L. E. Goodrich in *The Handbook of Porphyrin Science* (Eds.: K. M. Kadish, K. Smith, R. Guilard), World Scientific, Singapore, **2011**, p. 1; e) D. J. Stuehr, O. W. Griffith, In *Advances in enzymology and related areas of molecular biology, Vol. 65* (Ed.: F. F. Nord), Wiley, New York, **1992**, p. 287; f) C. Baciu, K.-B. Cho, J. W. Gauld, *J. Phys. Chem. B*

 © 2016 Wiley-VCH Verlag GmbH & Co. KGaA, Weinheim

2005, *109*, 1334; g) K.-B. Cho, M. A. Carvajal, S. Shaik, *J. Phys. Chem. B* **2009**, *113*, 336.

[3] a) J. S. Beckman, W. H. Koppenol, *Am. J. Physiol.* **1996**, *271*, C1424; b) R. Radi, *Proc. Natl. Acad. Sci. USA* **2004**, *101*, 4003; c) B. Kalyanaraman, *Proc. Natl. Acad. Sci. USA* **2004**, *101*, 11527; d) P. C. Dedon, S. R. Tannenbaum, *Arch. Biochem. Biophys.* **2004**, *423*, 12; e) S. Goldstein, J. Lind, G. Merényi, *Chem. Rev.* **2005**, *105*, 2457; f) P. Pacher, J. S. Beckman, L. Liaudet, *Physiol. Rev.* **2007**, *87*, 315; g) G. Ferrer-Sueta, R. Radi, *ACS Chem. Biol.* **2009**, *4*, 161; h) M. P. Schopfer, J. Wang, K. D. Karlin, *Inorg. Chem.* **2010**, *49*, 6267; i) N. L. Fry, P. K. Mascharak, *Acc. Chem. Res.* **2011**, *44*, 289; j) T. C. Berto, A. L. Speelman, S. Zheng, N. Lehnert, *Coord. Chem. Rev.* **2013**, *257*, 244; k) M.-L. Tsai, C.-C. Tsou, W.-F. Liaw, *Acc. Chem. Res.* **2015**, *48*, 1184; l) R. Pulukkody, M. Darensbourg, *Acc. Chem. Res.* **2015**, *48*, 2049; m) A. P. Hunt, N. Lehnert, *Acc. Chem. Res.* **2015**, *48*, 2117; n) J. Fitzpatrick, E. Kim, *Acc. Chem. Res.* **2015**, *48*, 2453; o) S. Hematian, I. Garcia-Bosch, K. D. Karlin, *Acc. Chem. Res.* **2015**, *48*, 2462.

[4] P. C. Ford, D. A. Wink, D. M. Stanbury, *FEBS Lett.* **1993**, *326*, 1.

[5] a) N. V. Blough, O. C. Zafiriou, *Inorg. Chem.* **1985**, *24*, 3502; b) T. Nauser, W. H. Koppenol, *J. Phys. Chem. A* **2002**, *106*, 4084.

[6] a) L. Qiao, Y. Lu, B. Liu, H. H. Girault, *J. Am. Chem. Soc.* **2011**, *133*, 19823; b) R. J. Singh, S. P. A. Goss, J. Joseph, B. Kalyanaraman, *Proc. Natl. Acad. Sci. USA* **1998**, *95*, 12912.

[7] P. Quint, R. Reutzel, R. Mikulski, R. McKenna, D. N. Silverman, *Free Radical Biol. Med.* **2006**, *40*, 453.

[8] B. A. Freeman, P. R. S. Baker, F. J. Schopfer, S. R. Woodcock, A. Napolitano, M. O'Ischia, *J. Biol. Chem.* **2008**, *283*, 15515.

[9] a) P. Moënne-Loccoz, *Nat. Prod. Rep.* **2007**, *24*, 610; b) T. Hino, Y. Matsumoto, S. Nagano, H. Sugimoto, Y. Fukumori, T. Murata, S. Iwata, Y. Shiro, *Science* **2010**, *330*, 1666.

[10] D. M. Kurtz, Jr., *Dalton Trans.* **2007**, 4115.

[11] a) P. R. Gardner, A. M. Gardner, L. A. Martin, A. L. Salzman, *Proc. Natl. Acad. Sci. USA* **1998**, *95*, 10378; b) H. Ouellet, Y. Ouellet, C. Richard, M. Labarre, B. Wittenberg, J. Wittenberg, M. Guertin, *Proc. Natl. Acad. Sci. USA* **2002**, *99*, 5902; c) P. C. Ford, I. M. Lorkovic, *Chem. Rev.* **2002**, *102*, 993; d) S. Herold, W. H. Koppenol, *Coord. Chem. Rev.* **2005**, *249*, 499.

[12] a) J. Lee, J. A. Hunt, J. T. Groves, *J. Am. Chem. Soc.* **1998**, *120*, 7493; b) R. Silaghi-Dumitrescu, *J. Mol. Struc. Theochem.* **2005**, *722*, 233; c) J. Su, J. T. Groves, *J. Am. Chem. Soc.* **2009**, *131*, 12979.

[13] K. J. Koebke, D. J. Pauly, L. Lerner, X. Liu, A. A. Pacheco, *Inorg. Chem.* **2013**, *52*, 7623.

[14] a) E. T. Yukl, S. de Vries, P. Moënne-Loccoz, *J. Am. Chem. Soc.* **2009**, *131*, 7234; b) T. S. Kurtikyan, P. C. Ford, *Chem. Commun.* **2010**, *46*, 8570.

[15] a) A. Yokoyama, J. E. Han, J. Cho, M. Kubo, T. Ogura, M. A. Siegler, K. D. Karlin, W. Nam, *J. Am. Chem. Soc.* **2012**, *134*, 15269; b) A. Yokoyama, K.-B. Cho, K. D. Karlin, W. Nam, *J. Am. Chem. Soc.* **2013**, *135*, 14900; c) A. Yokoyama, J. E. Han, K. D. Karlin, W. Nam, *Chem. Commun.* **2014**, *50*, 1742.

[16] S. Hong, K. D. Sutherlin, J. Park, E. Kwon, M. A. Siegler, E. I. Solomon, W. Nam, *Nat. Commun.* **2014**, *5*, 5440, DOI: 10.1038/ncomms6440.

[17] P. K. Wick, R. Kissner, W. H. Koppenol, *Helv. Chim. Acta* **2000**, *83*, 748.

[18] T. S. Kurtikyan, S. R. Eksuzyan, V. A. Hayrapetyan, G. G. Martirosyan, G. S. Hovhannisyan, J. A. Goodwin, *J. Am. Chem. Soc.* **2012**, *134*, 13861.

[19] a) C. G. Miller, S. W. Gordon-Wylie, C. P. Horwitz, S. A. Strazisar, D. K. Peraino, G. R. Clark, S. T. Weintraub, T. J. Collins, *J. Am. Chem. Soc.* **1998**, *120*, 11540; b) S. Hong, Y.-M. Lee, M. Sankaralingam, A. K. Vardhaman, Y. J. Park, K.-B. Cho, T. Ogura, R. Sarangi, S. Fukuzumi, W. Nam, *J. Am. Chem. Soc.* **2016**, *138*, 8523.

[20] It is worth noting that the peroxynitrite (PN) is often proven to be present by its ability to effect phenol-ring nitration. Thus, we carried out the reactions of **1** (and **2**) with nitric oxide in the presence of 2,4-di-*tert*-butylphenol (DTBP), which led to the production of 2,4-di-*tert*-butyl-6-nitrophenol in good yield (62% for **1** and 57% for **2**, respectively, see the Supporting Information). These results thus strongly support our proposed formation of metal–peroxynitrite species in the course of the nitric oxide oxygenation reaction. Also, see: Ref. [3g] and a) H. Gunaydin, K. N. Houk, *Chem. Res. Toxicol.* **2009**, *22*, 894.

Received: June 13, 2016
Revised: July 25, 2016
Published online: September 4, 2016

 © 2016 Wiley-VCH Verlag GmbH & Co. KGaA, Weinheim